International Virtual Conference on Materials and Nanotechnology
In Association with International Journal of Scientific Research in Science and Technology
Volume 9 | Issue 4 | Print ISSN: 2395-6011 | Online ISSN: 2395-602X (www.ijsrst.com)

Raman Spectroscopic Technique for Cancer Diagnosis

Patil S A[1], Thakare N R[1], Bhoyar A D[1]
[1]P. R. Pote College of Engineering and Management, Amravati, Maharashtra, India

ABSTRACT

Raman Spectroscopic technique can be applied for the cancer diagnosis as it can probe the molecular changes associated with diseased tissue. The molecular and cellular changes occurring in the disease result in distinct Raman Spectra. We have recorded the Raman Spectra of 4 samples at different positions. The Raman features and intensity differs for normal and malignant cells which can be attributed to the variation in the chemical composition of the cells.

Keywords : Raman Spectra, Cancer, Molecular Change

I. INTRODUCTION

Raman Spectroscopy is a vibrational spectroscopic technique that can be used to optically probe the molecular changes associated with diseased tissue. Early cancer detection and localization with effective treatment is crucial to increasing the survival rates. However because early cancers i.e. precancer such as dysplasia and carcinoma in situ (CIS) are only a few cell layer thick (0.2 to 1mm) they can be very difficult to visually detect by conventional diagnostic methods. Tissue fluorescence spectroscopy can be successfully used in vivo to diagnose early lung cancers.[1,2] But it has some draw back. Tissue auto fluorescence spectral features are broad and show less specific difference between normal and pathologic tissues. The Raman effect is an inelastic light scattering process whereby a small proportion of incident of photons are scattered with a corresponding change in frequency. The difference between the incident and scattered frequencies corresponds to the vibrational modes of molecules participating in the interaction. The presence of the neighbouring molecules also change the frequency, intensity and bandwidth of the scattered light and hence give information about the corresponding interaction.

Raman spectra are depicted by plotting the intensity of the scattered photons as a function of the frequency shift. Raman spectra can capture a finger print of specific molecular species and can therefore be potentially used for biomedical applications. Most biologic molecules are Raman active scatterers, each with its own spectral fingerprint Raman spectra usually exhibit sharp spectral features that are characteristic of specific molecular structures and confirmation of tissues[3,4] thus providing more specific molecular information about a given tissue or disease state. Raman spectroscopy is particularly amenable for in vivo analysis because the power and wavelength of the lasers used do not cause injury. Raman spectroscopy can provide information about

the conformation of macromolecules such as proteins, nucleic acid and lipids.

Near infrared Raman spectroscopy has certain advantages such as relative insensitivity to tissue water contents and deeper penetration depth in to the tissue.

That justify its increasing popularity for biomedical application.[5,6] In recent years NIR Raman spectroscopy has been investigated for invitro diagnosis of malignant tissue from various organs (e.g. brain, breast, bladder, colon, larynx, cervix and skin)[7-9] These studies show that specific features of tissue Raman Spectra can be related to the molecular and structural changes associated with neoplastic transformation.[10, 11]

II. DIFFERENCE BETWEEN RAMAN AND FLUORESCENCE SPECTROSCOPY

Raman Scattering and Fluorescence emission are 2 competing phenomena, which have similar origin. Generally a laser photon bounces off a molecule and looses a certain amount of energy that allows the molecule to vibrate (Stokes process). The scattered photon is therefore less energetic and associated light exhibits a frequency shift. The various frequency shifts associated with different molecular vibration gives rise to the spectrum that is characteristic of certain compound.

In contrast fluorescence or luminescence emission follows an absorption process. For better understanding one can refer to the diagram below.

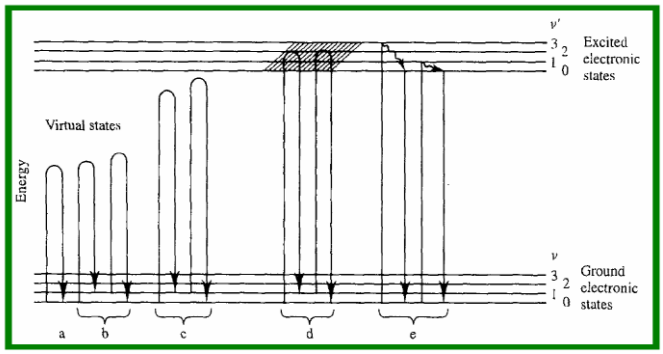

Figure 5(a) : Mechanisms of various light scattering processes. (a) Rayleigh, (b) nonresonance Raman, (c) pre-resonance Raman, (d) resonance Raman resonance fluorescence and (e) relaxed fluorescence.

Virtual states have to be considered to explain Raman Scattering. This is related to the fact that the interaction of the photon with the molecule and the re-emission of the scattered photon occur almost simultaneously. The existence of such virtual states also explains why the non-resonance Raman effect does not depend on the wavelength of the excitation, since no real states are involved in the interaction mechanism. In fact, the Raman spectrum generally does not depend on the laser excitation.

However when the energy of the excitation photon gets close to the transition energy between two electronic state one then deals with the resonance Raman or resonance fluorescence (Figure 1 cased (d)).

The basic difference between these two processes is related to the time scale involved, as well as with the nature of the so called intermediate states. In contrast with resonant fluorescence, relaxed fluorescence results from the emission of a photon from the lowest vibrational level of an excited electronic state, fallowing a direct absorption of a photon and relaxation of the molecule from its vibrational excited level of the electronic state back to the lowest vibrational level of the electronic state. A fluorescence process typically requires more than 10 Sec.[9] In contrary Raman transition is completed within a picoseconds or less.

It clearly appears that, depending on the laser wavelength, resonance effects (Raman or fluorescence), may or may not exist. If the excitation photon does not provide sufficient energy to the molecule, the required transition to generate fluorescence will not take place. However, if fluorescence is generated, it is often much more intense than Raman scattering, hiding Raman features. But because the Raman spectrum tends to be more informative than fluorescence, the Raman spectroscopist is continually searching for methods to avoid fluorescence.

One method to avoid fluorescence condition is to select the laser excitation wavelength. For most examples the choice of Near I.R. (NIR) or UV laser wave length can avoid exciting fluorescence. In the second case the fluorescence may be excited, but the emission is widely separated in energy from the Raman signal so that the Raman spectrum can be recorded without fluorescence interference.

Several biological molecules such as nucleic acids, proteins, and lipids have distinctive Raman features that yield structural and environmental information. These molecules have been studied in solutions and in their natural microscopic environments[11]. The molecular and cellular changes that occur with disease result in distinct Raman spectra that can be used for diagnosis. The transitional changes in precancerous tissues as well as benign abnormalities such as inflammation can also yield characteristic Raman features that allow their differentiation.

III. REVIEW OF LITERATURE

Several groups have indicated the potential of vibrational spectroscopy for disease diagnosis in various organ sites. These groups have shown that features of the vibrational spectrum can be related to molecular and structural changes associated with disease. Raman spectroscopy has been studied extensively for tissue diagnosis in four main organ sites; breast [12] esophagus[13] (and the GI tract), cervix (other gynecological tissues)[14] and skin[15].

Several groups have studied the potential of Raman spectroscopy for pathologies of the breast, from detection of breast cancers to study of capsules from breast implants. Using an FT-Raman system, Alfano et_al. obtained the 1st Raman spectra from excised normal human breast tissues and benign and malignant breast tumors and discussed the feasibility of using FT-Raman spectroscopy for different eating normal and malignant breast tissues.[10]

Redd et_al[16] employed Raman spectroscopy using visible excitation to study excised human breast tissues. Spectra were also obtained from pure compounds and the features observed in tissue spectra were determined to be primarily due to carotenoids myoglobin and lipids.

Feld and colleagues[6] have done extensive work on using Raman spectroscopy for breast cancer diagnosis.

FT-Raman spectroscopy of various gynecologic tissues was also first studied by Affano et_al. Characteristic Raman feature of normal tissues and malignant tumors from the cervix, uterus, endometrium and ovary were described.

A lot of work has been done in diagnosing skin cancer. A study exploring the use of confocal Raman microspectroscopy for skin cancer detection has also been reported.[11] Many researchers have applied NIR Raman Spectroscopy in vitro, exvivo as well as in vivo for the diagnosis of cancer with varying degree of successes.

There is indication that Raman spectroscopy is poised to follow through on its potential to provide real time, non-invasive, automated diagnosis of various cancers Although the process of developing automated classification algorithms has proved arduous, new cutting edge classification algorithms suggest that with enough data, this type of diagnosis will be soon possible.

Researchers also are beginning to understand the biological basis of Raman spectral differences between normal and malignant tissues with the help of techniques like spectral mapping and using tissue model systems. This would enable improved understanding of the progression of cancer.

IV. EXPERIMENTAL ARRANGEMENT

Different samples of tissues were collected and they were recorded using the laser Raman instrumentation. In this set up, a diode laser (785nm, l00mw) is used for excitation of the samples. The scattering is spectrum analyzed by HR320 spectrograph. The scattered radiation is detected by the intense radiation of nitrogen cooled CCD camera. A holographic filter

was used to filter the excitation source. A notch filter is used for removing the Raleigh scattering. Baseline corrected, smoothened, calibrated and normalized spectra (to the highest peak) were subjected to multivariate statistical analysis PC A for objective classification of normal, malignant and benign tissues.

The spectrograph used in the Raman spectrophotometer is highly specialized. The intensity of Rayleigh scattered light is about ten thousand times more than the Raman scattered light. The Raman lines may be obscured by the Rayleigh lines. In order to avoid the overlap of the lines two gratings have been employed in the design of spectrograph.

V. RESULT AND DISCUSSION

Raman scattering cross section is very small and therefore high power laser is utilized as the source of light. When laser radiation having a particular frequency is incident on the sample it undergoes Raman scattering as well as Rayleigh scattering. The Rayleigh scattering light is eliminated by the holographic notch plus filter and the Raman signal is detected by CCD and the spectra is displayed on the P.C.

We record the Raman spectra of 4 samples which are displayed in figures 5.6(a), 5.7(a), 5.8(a) and 5.9(a). We record spectra of normal sample and at 5 different positions of the malignant samples. Considering the degree of malignancy directly proportional to the height of the peak we display the degree of malignancy in Figure 5.6(d), 5.7(d), 5.8(d) and 5.9(d) of the samples 1, 2, 3 and 4 respectively.

From the graph of Raman scattered light it can be observed that the curve indicating the normal sample has more no. of peaks than cancerous sample. But the peaks of normal curve are at lower intensity whereas the peak of cancerous samples is at higher intensities.

Table 5.1 to 5.4 shows the wave numbers of each peak of both normal and cancerous tissue. To better understand the molecular basis of the observed Raman spectra, Table 5.5 lists tentative assignments for the observed Raman bands according to literature data. Thus distinctive Raman features and intensity differences for tumor verses normal tissue can reflect molecular and cellular changes associated with normal and malignant transformation. For instance let us consider graphs 5.6(a) the peak 1425 cm^{-1} in normal tissue can probably be attributed to collagen. However in malignant tissue collagen band was found to shift to 1445cm^{-1} The band at 1445 cm^{-1} are the characteristic of the CH_2-CH_3 bending modes of collagen and phospholipids and their intensities are high in cancerous tissue. Let us consider the example of graph 5.9(a). The peak at 1075 cm^{-1} in normal tissue can be attributed to v(c-c) as v(c-0) phospholipids. But in case of cancerous tissue this peak is shifted to 1087 cm^{-1}.

The observation of the figures 5.6(c) to 5.9(c) show that at the centre of the region the malignancy is maximum and as the point of observation moves away from the center the malignancy goes on decreasing.

The comparison between Raman spectra of two different breast cancer i.e. Figure 5.6(a) and 5.7(a) shows that the number of peaks observed in the spectra is different. Further it is seen that peaks are obtained at different positions showing that the two samples either differ in positions in the breast or they differ in degree of malignancy. The shift in the peak positions shows that the vibrational constant of the molecule change and therefore the neighboring situation is changed as the tissue transforms from normal to malignant condition.

VI. CONCLUSION

The position, intensity and shape of peaks in the Raman spectra of cancerous tissue were significantly different compared with those of normal tissues. From the above discussion it is clear that, the detail study of vibrational levels of Amino acid, structural proteins, and lipids may help in the study of the chemical composition morphology of tissue of cancerous as well as normal tissues.

The analysis of the experimental work suggests that the intensity mapping can be done in case of the Raman Spectra by using proper filters. The variation in the intensity ratio might help in the determination of degree of malignancy.

Continued development of Raman Spectroscopic instrumentation is needed to per format the level necessary for clinical use including the design of a complete hardware apparatus which is compact and can be easily integrated into the clinical setting.

Development of Raman instrumentation is also needed to make it reasonable so that it becomes affordable to the people.

If more Raman spectra are recorded and investigated the mechanism of progress of disease can be studied and the reasons behind the cancer of different organs can be found out.

The interaction between the tissues of the human organ with the external agencies and the effect produced by the external agencies may be explored. Depending upon the type of interaction between tissues and external agencies the people can be divided into different categories. The cancer prone people can be also be found out and they can also be divided into various categories.

Thus finally we may conclude based on the Raman spectra, we are able to discriminate normal versus cancer tissue and observe changes in signature Raman peak representing structural changes of macromolecules.

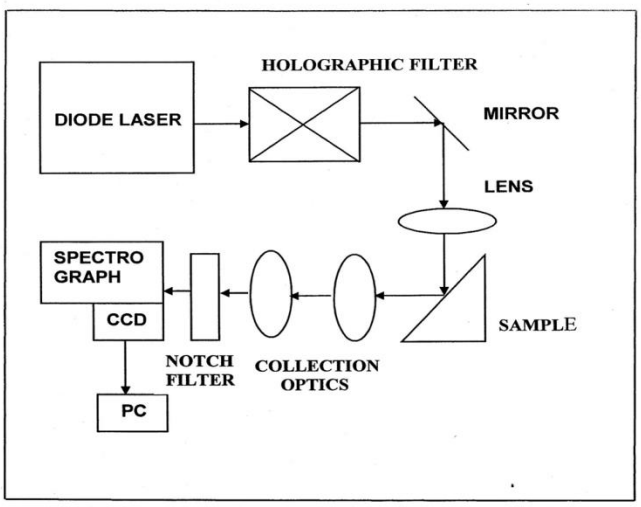

Figure 5(b): Block diagram of the Raman Spectrophotometer.

Table 5.1: The details about peaks in the Raman Spectra of Sample 1

Sr. No.	Peak No.	Normal Energy cm^{-1}	Cancer Energy cm^{-1}
1.	1	-	850
2.	2	-	1075
3.	3	1275	1300
4.	4	1425	1445
5.	5	1650	1650

Table 5.2: The details about peaks in the Raman Spectra of Sample 2

Sr. No.	Peak No.	Normal Energy cm^{-1}	Cancer Energy cm^{-1}
1.	1	825	850
2.	2	-	1100
3.	3	-	1275
4.	4	1450	1462
5.	5	1650	1670

Table 5.3: The details about peaks in the Raman Spectra of Sample 3

Sr. No.	Peak No.	Normal Energy cm^{-1}	Cancer Energy cm^{-1}
1.	1	827	850
2.	2	900	937.5
3.	3	-	1237
4.	4	1425	1450
5.	5	1637	1650

Table 5.4: The details about peaks in the Raman Spectra of Sample 4

Sr. No.	Peak No.	Normal Energy cm^{-1}	Cancer Energy cm^{-1}

1.	1	-	850
2.	2	-	937
3.	3	1075	1087
4.	4	-	1312
5.	5	1412	1450
6.	6	1637	1662

Table 5.5: Peak positions and tentative assignments of major vibrational Bands observed in normal and Tumor bronchial tissue.

Peak position (Cm^{-1})	Protein assignments	Lipid assignments	Others
1745w		v(c=o) gnmento v(c=o) phopholipids	
1655 vs	v(c=o) amid1, x-helix, collagen, elastin		
1618S(sh)	v(c=c), tryptophan		v(c=c), paphyrin
1602ms(sh)	δ(c=c), phenylalanine		
1582 ms(sh)	δ(c=c), phenylalanine		
1552ms (sh)	v(c=c), tryptophan		v(c=c) porphyrin v(c=c), carotenoid
1445vs	$\delta(CH_2)$, $\delta(CH_3)$,	$\delta(CH_2)$ serssoring,	
	Collagin	phospholipids	
1335(sh)	Ch_3CH_2 wagging, collagen		Ch_3CH_2 wagging, nudric acid
1322s	Ch_3CH_2 twisting, collogen		
1302vs	δ (CN), δ(NH) twisting, wagging, collagen	δ(c+b) twisting, wagging phospholipids	
1265s(sh)	δ (CN), δ(NH) amide III, x-helix, collagen, tryptophan.		
1223mw(sh)			Vas(Po2), nudlic acids
1208w(sh)	v(c=c6h_5), tryptophan, phenylalanine		
Peak position (Cm^{-1})	Protein assignments	Lipid assignments	Others
Peak position (Cm^{-1})	Protein assignments	Lipid assignments	Others
1172vw	δ(C-H), tyroscine		
1152w	v(c-N), proteins		

1123w	v(c-N), proteins		
1078ms		v(c-c) or v(c-o), phospholipids	
1031mw(sh)	δ(C-H), phenylolin e		
1004ms	vs(c-c), symm etricring breathing, phenylaline.		
963w	unassigned		
935w	v(c-c), x-helix, praline, valine		
876w(sh)	v(c-c), praline δ(CCH) ring breathing tyrosine		Polysaccharide
823w	Out of plane ring breathing, tyrosine		
752w	Symmetric breathing tryptophan.		

v, stretching mode, vs, symmetric stretch, vas, asymmetric stretch, δ bending mods, v, very, s, strong, m, medium, w, weak, sh, shoulder.

VII. REFERENCES

[1]. Lam S, Kennedy T, Urger M. Miller YE, Germont D, Rusch V, "Localization of bronchial intraepithelial neoplastic usionsty fluorescence bronchioscopy", (1998)

[2]. Hung J, Lam S, Le Riche JC, Palcic B, "Autofluorence of normal and Malignant bronchial tissue, Laser Surg." Med. (1991)

[3]. Peno JR, Grygon CA, Spiro TG, "Raman Excitation Profiles for the nucleotides and for the nudlic acid duplexes poly (rA)-poly (rU) and poly (dG-dC) J. Physchon" (1989) V93.

[4]. Tu AT, Peptide backbone conformation and microenvironment of Pritein side chain. "Spectroscopy of biological Systems", New York John Willey and Sons, (1986)

[5]. Frank CJ, McCreery R/s, Redd-DC, Raman Spectroscopy of normal and diseased human breast tissues. Anal Chem. 1995, 67.

[6]. Manocharan R, Shafer K, Perelmon L, Wu J, Chen K, Denium G, Fitzmarice M, Myles J, Crowe J, Darari R, Fold MS, "Raman Spectroscopy and fluorescence photon migration for breast cancer diagnosic and imaging" Photochem Photobio, (1998), 67, 15-22.

[7]. Schrader B, Keller S, Loechte T, Fendels, Moore DS, Simon A, Sawatzki J., NIRFT Raman Spectroscopy in medical diagnosis. J. Mol Struct (1995), DP 348-293-6.

[8]. Mahadevan-Jansen A, Mitchell MF, Ramanujan N, Malpica A, Thomsen S, Utzinger J, Richard Kortum R. Near infrared Raman spectroscopy for in vitro detection of cervical precanars. Photochem Photobio. (1998) 68.

[9]. Lau DP, Hang Z, Luitl, MonCS, Poerean K, Morrison MD, Zeng H, "Raman spectroscopy for early detection of laryngeal malignancy : preliminary result, Laryngoscope (2000), 110.

[10]. Alfano RR, Liu CH, Sha WL, Zhu D, Akins L, "Human breast tissues studied by IR Flowerer transform Raman Spectroscopy" Lasers Life Sci.(1991).

[11]. Mahadevan Gansen A, Richards Kortum R, "Raman Spectroscopy for the detection of cancer and precancer "J Biomed Opt. (1996).

[12]. Shafer-Pettier, K.E. Haka, A.S. Fitzmauria, M, Crowe J., Myles J., Dasari R.R. and Feld M.S. "Raman Micro spectroscopic model of human breast tissue, implications for breast cancer diagnosis in vivo", J.Raman Spectros. 33 (2002).

[13]. Stone N., Kendall C., Shepherd N., Crow P., Bars H., "Near-infrared Raman Spectroscopy for the classification of epithelial pre-can as and cancers", J.Raman Spectrosc, 33, 564, 2002.

[14]. Utginger U., Heintzelman D.L., Mahadevan Gansen A., Malpica A., Follen M. and Richards Kortum, "NTR spectroscopy for in vivo detection of cervical precancers", Appl. spectrosc. 55, 955 (2001).

[15]. Nijssen A, Bakker Schut, T.C. Heuls F., Caspers P.J., Hayes D.P., Neumann M.H., and Puppels G.J., "Discriminating basal cell carcinoma from its surrounding tissue by Raman spectroscopy, J.Invest. Dermatot, 119, 64, 2002.

[16]. Trans R.C.M, McCrery R.L. and Redd D.C. "Raman spectroscopy of normal and diseased human breast tissues, "Anal.Chem, 67, 777, 1995.

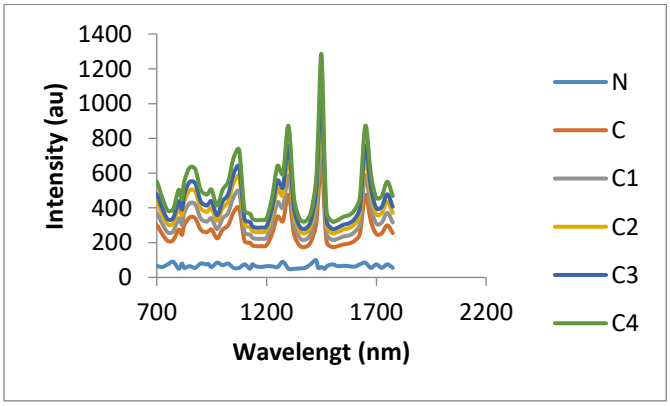

Figure (5.6a) Intensity of Raman scattered light as a function of energy (sample 1)

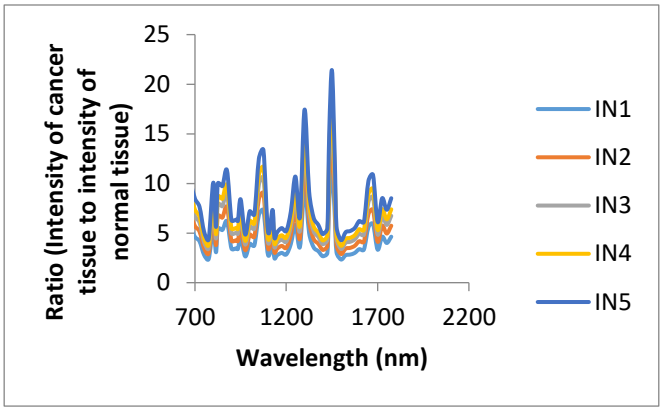

Figure (5.6b) Ratio of intensity of Raman scattered light as a function of energy (sample 1)

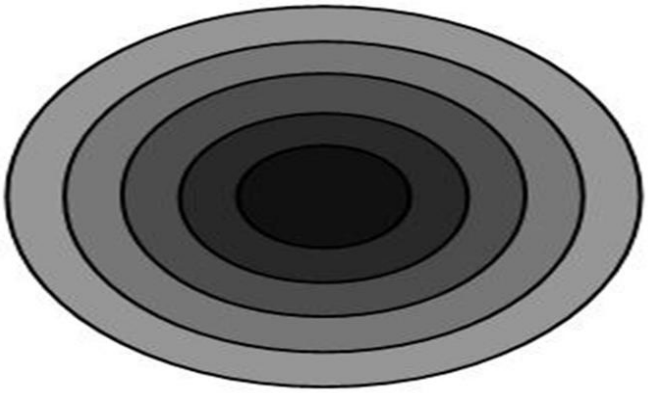

Figure (5.6c) spatial distribution of fluorescence intensity at peak wavelength

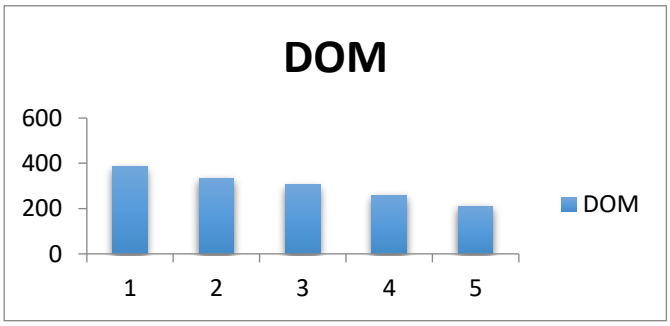

Figure (5.6d) spatial variation of degree of malignancy (sample 1)

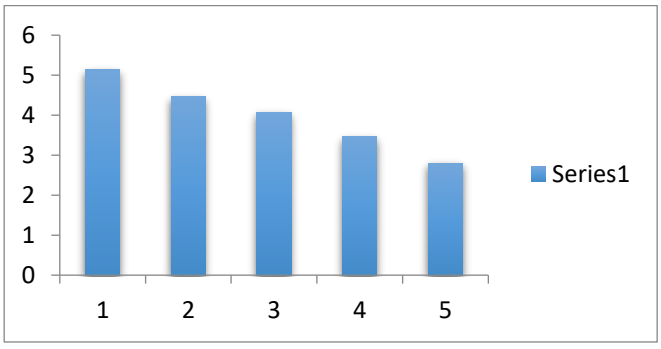

Figure (5.6e) spatial variation of ratio of intensity (sample 1)

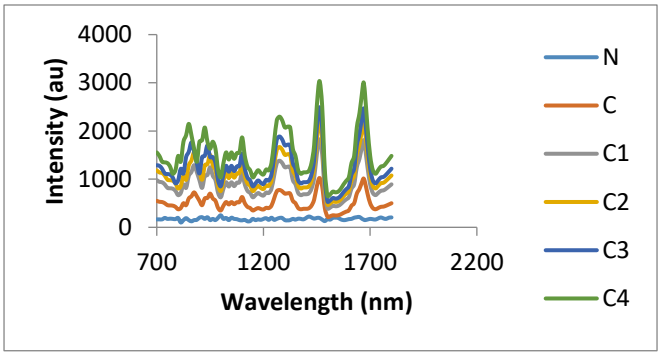

Figure (5.7a) Intensity of Raman scattered light as a function of energy (sample 2)

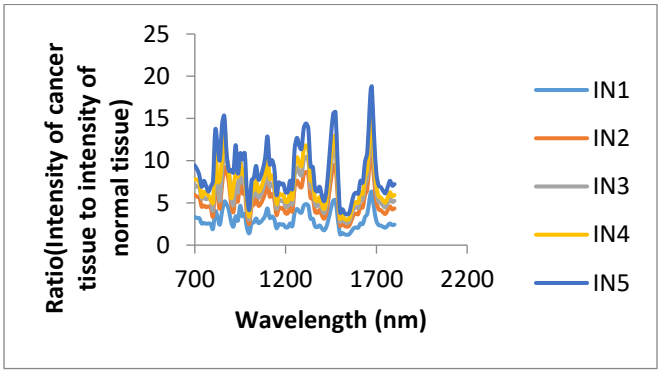

Figure (5.7b) Ratio of intensity of Raman scattered light as a function of energy (sample 2)

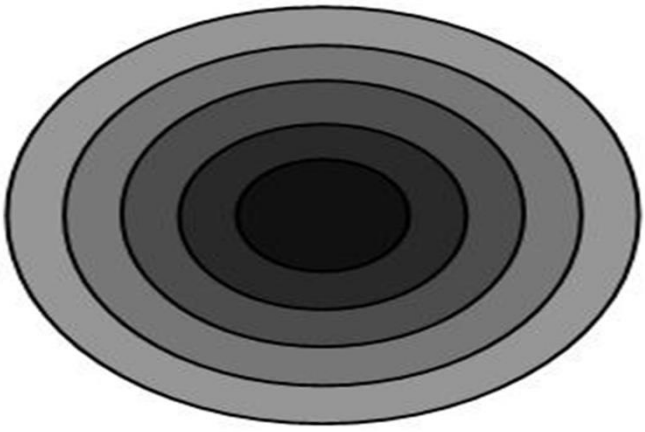

Figure (5.7c) spatial distribution of fluorescence intensity at peak wavelength

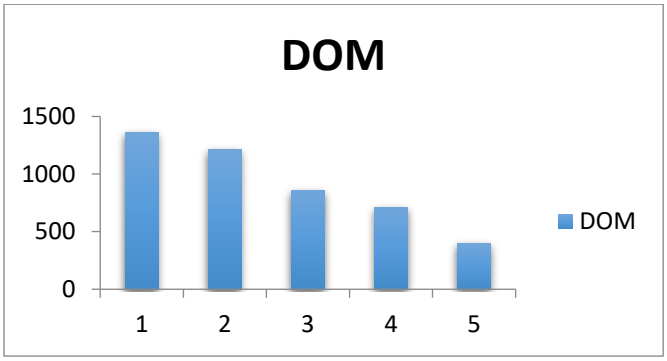

Figure (5.7d) Spatial variation of degree of malignancy (sample 2)

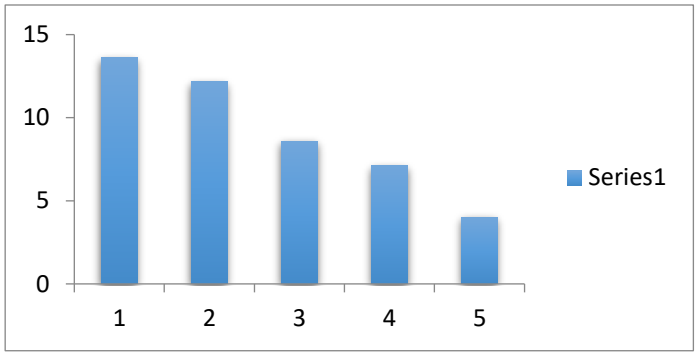

Figure (5.7e) spatial variation of ratio of intensity (sample 2)

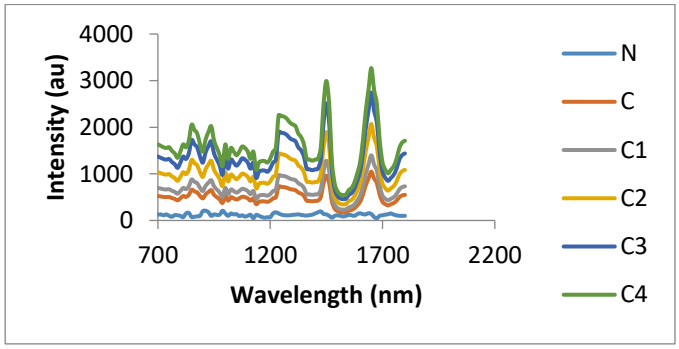

Figure (5.8a) Intensity of Raman scattered light as a function of energy (sample 3)

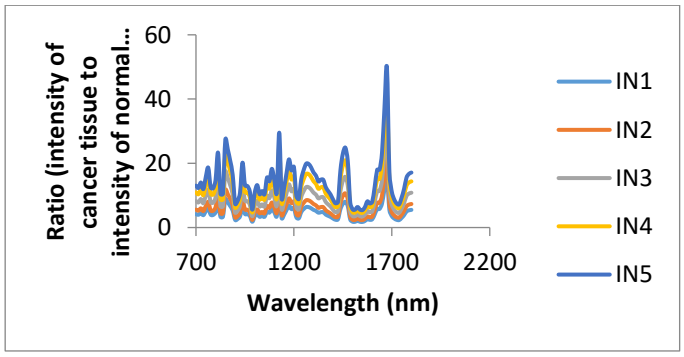

Figure (5.8b) Ratio of intensity of Raman scattered light as a function of energy (sample 3)

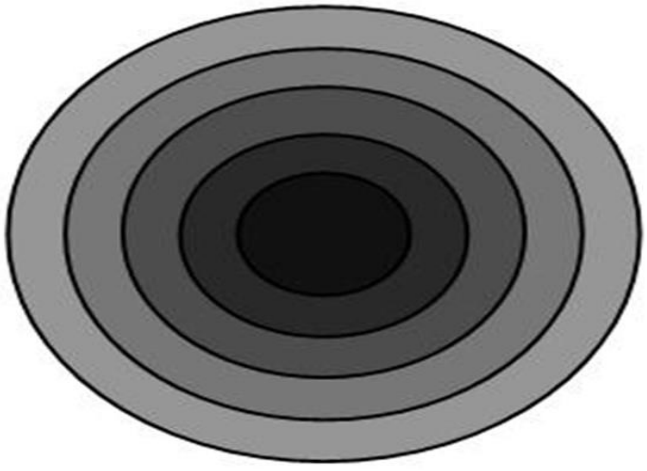

Figure (5.8c) spatial distribution of fluorescence intensity at peak wavelength

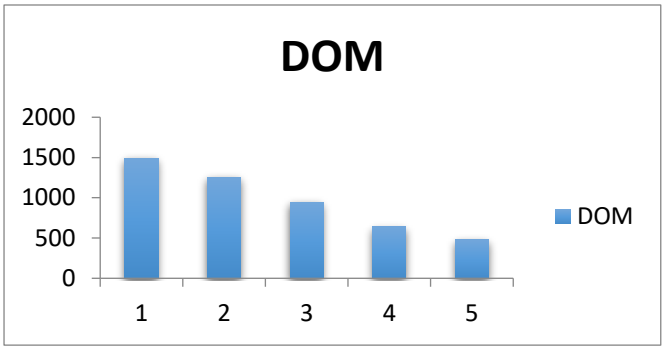

Figure (5.8d) spatial variation of degree of malignancy (sample 3)

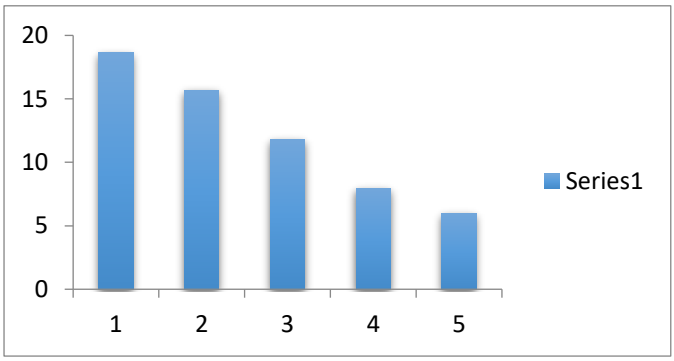

Figure (5.8e) Spatial variation of ratio of intensity (sample 3)

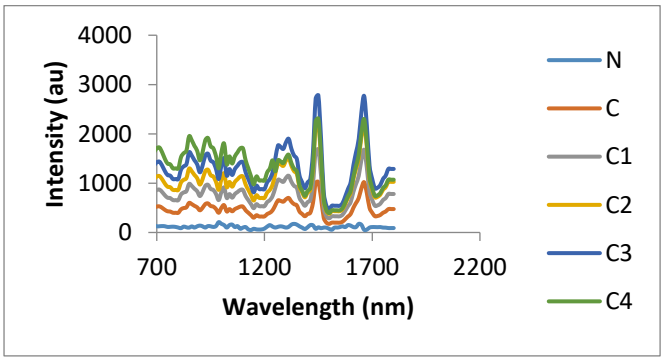

Figure (5.9a) Intensity of Raman scattered light as a function of energy (sample 4)

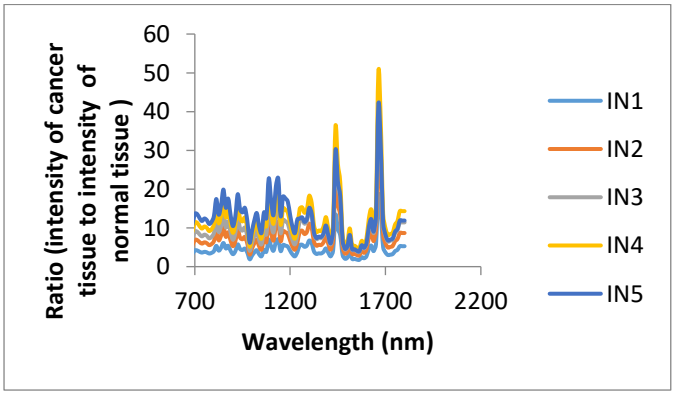

Figure (5.9b) Ratio of intensity of Raman scattered light as a function of energy (sample 4)

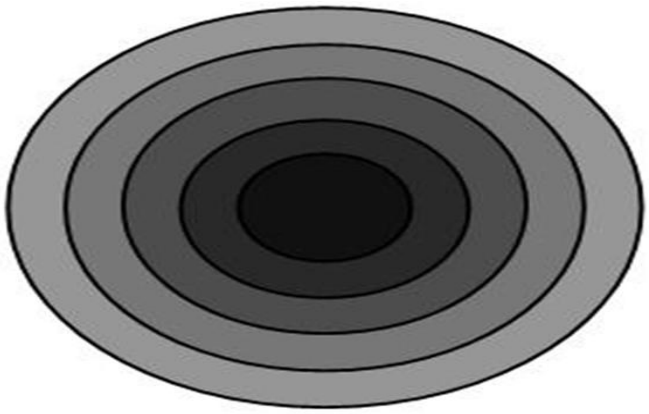

Figure (5.9c) Spatial distribution of fluorescence intensity at peak wavelength

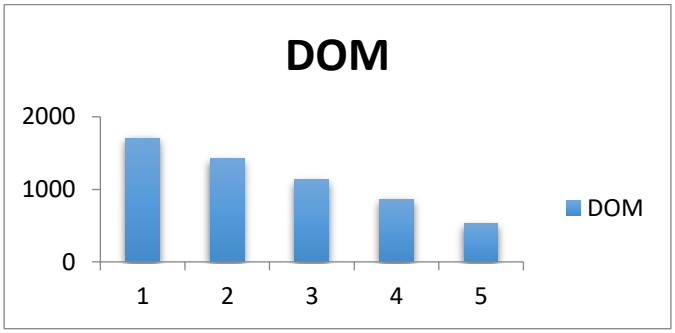

Figure (5.9d) Spatial variation of degree of malignancy (sample 4)

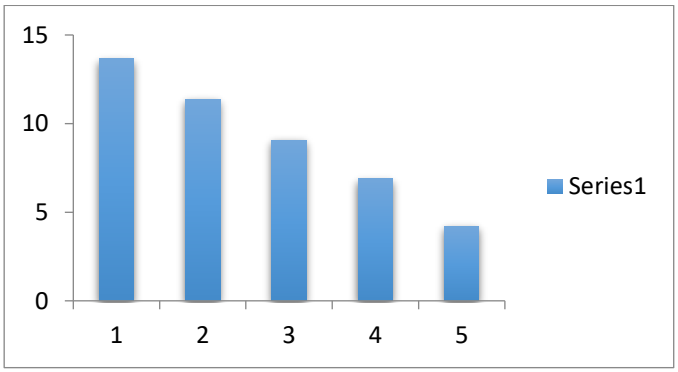

Figure (5.9e) Spatial variation of ratio of intensity (sample 4)